Proceedings of the ASME 2013 International Design Engineering Technical Conferences & Computers and Information in Engineering Conference
IDETC/CIE 2013
August 12-15, 2013, Portland, OR, USA

DETC2013-12151

IS THERE AN OPTIMAL CHOICE OF CONFIGURATION SPACE FOR LIE GROUP INTEGRATION SCHEMES APPLIED TO CONSTRAINED MBS?

Andreas Müller[1], **Zdravko Terze**[2]
[1] Institute of Mechatronics, Reichenhainer Str. 88, 09126 Chemnitz, Germany, andreas.mueller@ifm-chemnitz.de
[2] University of Zagreb, Croatia, Email: zdravko.terze@fsb.hr

ABSTRACT

Recently various numerical integration schemes have been proposed for numerically simulating the dynamics of constrained multibody systems (MBS) operating. These integration schemes operate directly on the MBS configuration space considered as a Lie group. For discrete spatial mechanical systems there are two Lie group that can be used as configuration space: $SE(3)$ and $SO(3)\times\mathbb{R}^3$. Since the performance of the numerical integration scheme clearly depends on the underlying configuration space it is important to analyze the effect of using either variant. For constrained MBS a crucial aspect is the constraint satisfaction. In this paper the constraint violation observed for the two variants are investigated. It is concluded that the $SE(3)$ formulation outperforms the $SO(3)\times\mathbb{R}^3$ formulation if the absolute motions of the rigid bodies, as part of a constrained MBS, belong to a motion subgroup. In all other cases both formulations are equivalent. In the latter cases the $SO(3)\times\mathbb{R}^3$ formulation should be used since the $SE(3)$ formulation is numerically more complex, however.

Keywords– Constrained multibody systems, Lie group integration, screw systems

1 Introduction

Lie group integration schemes for MBS commonly rest on $SO(3)\times\mathbb{R}^3$ as configuration space manifold. This configuration space cannot capture the intrinsic geometry of rigid body motions since it does not represent proper screw motions. Moreover the general motion of a rigid body is a screw motion. This applies to unconstrained as well as constrained rigid bodies, and the reconstruction of finite motions within numerical time stepping schemes shall take this into account. Along this line the Lie group $SE(3)$ of proper rigid body motions was recently used as configuration space [3], [4], [14]. It turned out that the proper rigid body motion group does outperform the standard $SO(3)\times\mathbb{R}^3$ formulation for a rigid bodies constrained to move relative to a stationary reference (e.g. heavy top), The obvious question is whether this statement applies to general constrained MBS, and whether there is an optimal choice for a given MBS that leads to the best numerical performance. In this paper two Lie group formulations for constrained MBS are compared and the effect of using either configuration space is analyzed for several examples.

In Lie group setting the dynamics of a constrained multibody system (MBS) is governed by the constrained Boltzmann-Hamel equations

$$\mathbf{M}(q)\dot{\mathbf{V}}+\mathbf{J}^T\lambda = \mathbf{Q}(q,\mathbf{V},t) \tag{1a}$$
$$\dot{q} = q\mathbf{V} \tag{1b}$$
$$\mathbf{g}(q) = \mathbf{0} \tag{1c}$$

where $q\in G$ represents the MBS configuration and G is the configuration space Lie group. This is an index 3 DAE system on the Lie group G. The system (2a) represents the motion equations of the MBS subjected to the geometric constraints (2c) that are complemented by the *kinematic reconstruction equations* (2b). That is, integration of (2b) yields the motion $\mathbf{q}(t)$ of the MBS corresponding to the MBS velocity $\mathbf{V}\in\mathfrak{g}$, with $\mathfrak{g}$ being the Lie algebra of G. In order to apply Lie group ODE integration schemes the first step is the reformulation of (2) as ODE on the state space $S:=G\times\mathfrak{g}$. This is achieved with the widely used index 1 formulation

$$\begin{pmatrix}\mathbf{M} & \mathbf{J}^T\\ \mathbf{J} & \mathbf{0}\end{pmatrix}\begin{pmatrix}\dot{\mathbf{V}}\\ \lambda\end{pmatrix}=\begin{pmatrix}\mathbf{Q}\\ \eta\end{pmatrix} \tag{2}$$

using the acceleration constraints $\mathbf{J}(q)\cdot\dot{\mathbf{V}}=\eta(q,\mathbf{V})$. This system replaces the dynamic equations (2a) when subject to the holonomic constraints (2c) since, for a given state $X=(q,\mathbf{V})\in S$, the system (2) and thus (2) can be solved for $\dot{\mathbf{V}}$ consistent with the acceleration constraints. The index reduction is achieved on the expense of numerical drifts of the constraints, however [1]. The overal ODE system is obtained by complimenting (2) with the kinematic equations (2b).

As far as the MBS model is concerned the numerical performance, and eventually the accuracy of any integration scheme whatsoever, are determined by 1) the choice of generalized coordinates and 2) by how generalized velocities are introduced. The first issue has to do with finding a proper chart on the configuration space, whereas the latter concerns the relation of velocities and time derivatives of the configurations, i.e. the relation (2b). The best solution for the first issue is to avoid local coordinates at all. The Lie group concept provides such a geometric vehicle that allows for coordinate-free modeling of frame transformations, where either $SO(3)\times\mathbb{R}^3$ or $SE(3)$ can be used. The second issue concerns the particular configuration space Lie group, noting that $q\in G$ and $\mathbf{V}\in\mathfrak{g}$.

The integration method considered in this paper is the Munthe-Kaas method. Since the kinematic reconstruction is inherent to the model the considerations shall apply to Lie group integration schemes in general.

2 Two State Spaces for Rigid Bodies

The configuration of a rigid body, with respect to a space-fixed inertial reference frame, is described by the position vector $\mathbf{r}\in\mathbb{R}^3$ of the origin of a body-fixed reference frame and its rotation matrix $\mathbf{R}\in SO(3)$, summarized by the pair $C=(\mathbf{R},\mathbf{r})$. A rigid body motion is thus a curve $C(t)$. The crucial point is to assign the Lie group C is living in. The state space is then the product of this Lie group and its Lie algebra.

2.1 Group of Proper Rigid Body Motions $SE(3)$

$SE(3)$ represents frame transformations, i.e. the combination of two successive rigid-body comfigurations are given by $C_2\cdot C_1=(\mathbf{R}_2\mathbf{R}_1,\mathbf{r}_2+\mathbf{R}_2\mathbf{r}_1)$. This multiplication rule indicates that $SE(3):=SO(3)\ltimes\mathbb{R}^3$ is the 6-dimensional semidirect product group of the rotation group $SO(3)$ and the translation group, represented as $\mathbb{R}^3$. Rigid body configurations can be represented in matrix form as

$$\mathbf{C}=\begin{pmatrix}\mathbf{R} & \mathbf{r}\\ \mathbf{0} & 1\end{pmatrix} \tag{3}$$

which admits representing the group multiplication as matrix multiplication

$$\mathbf{C}_2\mathbf{C}_1=\begin{pmatrix}\mathbf{R}_2\mathbf{R}_1 & \mathbf{r}_2+\mathbf{R}_2\mathbf{r}_1\\ \mathbf{0} & 1\end{pmatrix}. \tag{4}$$

A generic motion of a rigid body is a screw motion, i.e. an interconnected rotation and translation along a screw axis [2].
The velocity corresponding to the screw motion of a rigid body is a twist $\mathbf{V}=(\omega,\mathbf{v})\in\mathbb{R}^6$ with angular velocity ω and linear velocity vector $\mathbf{v}$. The *body-fixed twist* of a rigid body motion $\mathbf{C}(t)$ is determined as

$$\widehat{\mathbf{V}}:=\mathbf{C}^{-1}\dot{\mathbf{C}}\quad\text{with}\quad\widehat{\mathbf{V}}=\begin{pmatrix}\widehat{\omega} & \mathbf{v}\\ \mathbf{0} & 0\end{pmatrix}\in se(3) \tag{5}$$

where $se(3)$ is the Lie algebra of $SE(3)$. The assignment (5) is a one-one correpsondance of twist coordinate vectors and $se(3)$-matrices. $\widehat{\omega}:=\mathbf{R}^T\dot{\mathbf{R}}\in so(3)$ is the skew symmetric cross product matrix associated to the vector ω. Via this isomorphism the Lie bracket on $se(3)$, in vector representation, is given the screw product $[\mathbf{V}_1,\mathbf{V}_2]=(\omega_1\times\omega_2,\omega_1\times\mathbf{v}_2-\omega_2\times\mathbf{v}_1)$ [2]. For convenience $\omega\in so(3)$ is written for a vector $\omega\in\mathbb{R}^3$ to indicate that isomorphism of $so(3)$ and $\mathbb{R}^3$ equipped with the cross product as Lie bracket.
For any screw $\mathbf{X}=(\omega,\mathbf{v})\in\mathbb{R}^6$ with screw axis parallel to ω the linear part can be expressed with a position vector $\mathbf{r}$ on the screw axis as $\mathbf{v}=\mathbf{r}\times\omega+h\omega$. The screw $\mathbf{X}$ describes an instantaneous screw motion, i.e. a rotation about the axis ω together with a translation along this axis, where $h:=\omega\cdot\mathbf{v}/\|\omega\|$ is the pitch of the screw. If $h=0$, then $\mathbf{X}$ are simply the Plücker coordinates of a line parallel to the screw axis.
The Lie bracket can be expressed by a linear operation on screw coordinate vectors as $[\mathbf{V}_1,\mathbf{V}_2]=\mathbf{ad}_{\mathbf{V}_1}\mathbf{V}_2$ given by the matrix

$$\mathbf{ad}_{\mathbf{V}}=\begin{pmatrix}\widehat{\omega} & 0\\ \widehat{\mathbf{v}} & \widehat{\omega}\end{pmatrix}. \tag{6}$$

The connection between an infinitesimal screw motion $\mathbf{X}(t)$ and the correponding finite screw motion is given by the exponential mapping on $SE(3)$, which reads explicitly

$$\mathbf{X}=(\omega,\mathbf{v})\longmapsto\exp\widehat{\mathbf{X}}=\begin{pmatrix}\exp\widehat{\omega} & (I-\exp\widehat{\omega})(\omega\times\mathbf{v})+h\,\omega\\ 0 & 1\end{pmatrix} \tag{7}$$

where

$$\exp\widehat{\omega}=\mathbf{I}+\frac{\sin\|\omega\|}{\|\omega\|}\widehat{\omega}+\frac{1-\cos\|\omega\|}{\|\mathbf{X}\|}\widehat{\omega}^2 \tag{8}$$

is the exponential mapping on $SO(3)$. Important for the Lie group integration scheme is the differential of the exponential mapping, $\mathrm{dexp} : se(3) \times se(3) \to se(3)$ that can be introduced as $\mathrm{dexp}_{\widehat{\mathbf{X}}}\dot{\widehat{\mathbf{X}}} = \dot{\mathbf{C}}\mathbf{C}^{-1}$, with $\mathbf{C} = \exp\widehat{\mathbf{X}}$. Its signinifcance becomes clear by replacing $\mathbf{X}$ with $-\mathbf{X}$, which allows expressing the body-fixed twist as $\widehat{\mathbf{V}} = \mathrm{dexp}_{-\widehat{\mathbf{X}}}\dot{\widehat{\mathbf{X}}}$. The numerical ODE integration methods require the inverse of the dexp map. In vector representation of twists the inverse of dexp on $SE(3)$ is [13]

$$\mathrm{dexp}^{-1}_{\widehat{\mathbf{X}}} = \mathbf{I} - \frac{1}{2}\mathbf{ad}_{\mathbf{X}} + \left(\frac{2}{\|\omega\|^2} + \frac{\|\omega\| + 3\sin\|\omega\|}{4\|\omega\|(\cos\|\omega\| - 1)}\right)\mathbf{ad}^2_{\mathbf{X}} + \left(\frac{1}{\|\omega\|^4} + \frac{\|\omega\| + \sin\|\omega\|}{4\|\omega\|^3(\cos\|\omega\| - 1)}\right)\mathbf{ad}^4_{\mathbf{X}} \tag{9}$$

with $\mathbf{X} = (\omega, \mathbf{v})$. In vector representation of $so(3)$ the inverse of the differential of the exp mapping (8) for $\mathbf{R} = \exp\xi$ is given as matrix [6]

$$\mathrm{dexp}^{-1}_{\xi} = \mathbf{I} - \frac{1}{2}\widehat{\xi} + \left(1 - \frac{\|\xi\|}{2}\cot\frac{\|\xi\|}{2}\right)\frac{\widehat{\xi}^2}{\|\xi\|^2}. \tag{10}$$

The state of a single unconstrained rigid body is represented by the couple $(\mathbf{C}, \mathbf{V}) \in SE(3) \times se(3)$. The acceleration of the body is the time derivative $\dot{\mathbf{V}} \in \mathbb{R}^6$. Making use of (5) the time derivative of $\mathbf{C}$ can be identified with $\mathbf{V}$. The time derivative of the rigid body state $(\mathbf{C}, \mathbf{V})$ is thus isomorphic to $(\widehat{\mathbf{V}}, \dot{\mathbf{V}}) \in se(3) \times \mathbb{R}^6$. Consequently, in $SE(3)$ representation, the state space of a rigid body is the Lie group $SE(3) \times \mathbb{R}^6$ with Lie algebra $se(3) \times \mathbb{R}^6$. The multiplication on this rigid body state space is

$$(\mathbf{C}_1, \mathbf{V}_1) \cdot (\mathbf{C}_2, \mathbf{V}_2) = (\mathbf{C}_1\mathbf{C}_2, \mathbf{V}_1 + \mathbf{V}_2). \tag{11}$$

Being a Lie group the state space possesses an exponential mapping given by

$$\begin{array}{rccc} \exp: & se(3) \times \mathbb{R}^6 & \to & SE(3) \times \mathbb{R}^6 \\ & (\widehat{\mathbf{V}}, \mathbf{A}) & \mapsto & (\exp\widehat{\mathbf{V}}, \mathbf{A}) \end{array} \tag{12}$$

with the exponential (7). The rigid body state can thus be reconstructed from its time derivative via this exponential mapping. With the Lie bracket on the algebra $se(3) \times \mathbb{R}^6$

$$[(\widehat{\mathbf{V}}_1, \mathbf{A}_1), (\widehat{\mathbf{V}}_2, \mathbf{A}_2)] = ([\widehat{\mathbf{V}}_1, \widehat{\mathbf{V}}_2], \mathbf{0}) \tag{13}$$

the differential of the exponential mapping is

$$\mathrm{dexp}_{(\widehat{\mathbf{V}}_1, \mathbf{A}_1)}(\widehat{\mathbf{V}}_2, \mathbf{A}_2) = (\mathrm{dexp}_{\widehat{\mathbf{V}}_1}\widehat{\mathbf{V}}_2, \mathbf{A}_2). \tag{14}$$

2.2 Direct Product Group $SO(3) \times \mathbb{R}^3$

Neglecting the interrelation of rotations and translations the multiplication is

$$C_1 \cdot C_2 = (\mathbf{R}_1\mathbf{R}_2, \mathbf{r}_1 + \mathbf{r}_2) \tag{15}$$

which indicates that $C = (\mathbf{R}, \mathbf{r}) \in SO(3) \times \mathbb{R}^3$. The direct product $SO(3) \times \mathbb{R}^3$ is commonly used as rigid body configuration space for Lie group methods [3, 4, 7, 9, 14]. Apparently this multiplication does not represent frame transformations. The inverse element is $C^{-1} = (\mathbf{R}^T, -\mathbf{r})$.

The Lie algebra of the direct product $SO(3) \times \mathbb{R}^3$ is $so(3) \times \mathbb{R}^3$ with Lie bracket

$$[\mathbf{X}_1, \mathbf{X}_2] = (\omega_1 \times \omega_2, \mathbf{0}). \tag{16}$$

The exponential mapping on the direct product group is

$$\mathbf{X} = (\omega, \mathbf{v}) \longmapsto \exp\mathbf{X} = (\exp\widehat{\omega}, \mathbf{v}) \tag{17}$$

with the exponential mapping (8) on $SO(3)$. The dexp mapping is accordingly

$$\mathrm{dexp}_{(\xi, \mathbf{u})}(\eta, \mathbf{v}) = (\mathrm{dexp}_{\xi}\eta, \mathbf{v}), \tag{18}$$

with dexp mapping on $SO(3)$. Its inverse is readily $\mathrm{dexp}^{-1}_{(\xi, \mathbf{u})}(\eta, \mathbf{v}) = (\mathrm{dexp}^{-1}_{\xi}\eta, \mathbf{v})$.

The velocity of a rigid body is, with configuration $C \in SO(3) \times \mathbb{R}^3$, given as

$$(\widehat{\omega}, \mathbf{v}^s) = (\mathbf{R}^T\dot{\mathbf{R}}, \dot{\mathbf{r}}) := C^{-1}\dot{C} \in so(3) \times \mathbb{R}^3 \tag{19}$$

and in vector notation denoted $\mathbf{V} = (\omega, \mathbf{v}^s) \in \mathbb{R}^3 \times \mathbb{R}^3$, with $\mathbf{v}^s = \dot{\mathbf{r}}$. This velocity couple is clearly not a proper twist but contains a mix of body-fixed angular velocity ω and spatial linear velocity $\mathbf{v}^s$. It is therefore called *hybrid representation* of rigid body velocities [5], [12]. It is frequently used for expressing the Newton-Euler equations. Even though, angular and linear velocities are treated independently, and this definition does not reflect the intrinsic characteristics of screw motions.

In hybrid representation the state of a rigid body is represented by $(C, \mathbf{V}) \in SO(3) \times \mathbb{R}^3 \times so(3) \times \mathbb{R}^3$. This is a Lie group with algebra $so(3) \times \mathbb{R}^3 \times \mathbb{R}^6$. Multiplication is defined as

$$(C_1, \mathbf{V}_1) \cdot (C_2, \mathbf{V}_2) = (C_1 \cdot C_2, \mathbf{V}_1 + \mathbf{V}_2), \tag{20}$$

and the exponential mapping is, with (17),

$$\begin{array}{rccc} \exp: & so(3)\times\mathbb{R}^3\times\mathbb{R}^6 & \to & SO(3)\times\mathbb{R}^3\times\mathbb{R}^3\times\mathbb{R}^3 \\ & (\mathbf{V},\mathbf{A}) & \mapsto & (\exp\mathbf{V},\mathbf{A})\,. \end{array} \tag{21}$$

The Lie bracket is on this algebra is

$$[(\mathbf{V}_1,\mathbf{A}_1),(\mathbf{V}_2,\mathbf{A}_2)] = ([\mathbf{V}_1,\mathbf{V}_2],\mathbf{0}). \tag{22}$$

The differential of the exponential mapping is, with (18), given by

$$\mathrm{dexp}_{(\mathbf{V}_1,\mathbf{A}_1)}(\mathbf{V}_2,\mathbf{A}_2) = (\mathrm{dexp}_{\mathbf{V}_1}\mathbf{V}_2,\mathbf{A}_2). \tag{23}$$

3 State Space of MBS

3.1 Group of Proper Rigid Body Motions $SE(3)$

The configuration of an MBS consisting of n rigid bodies is represented by $q = (\mathbf{C}_1,\ldots,\mathbf{C}_n) \in G^{\ltimes}$, where

$$G^{\ltimes} := SE(3)^n \tag{24}$$

is the $6n$-dimensional configuration space Lie group. This is a coordinate-free representation of MBS configurations. The multiplication on $G^{\ltimes}$ is understood componentwise, and thus $q^{-1} = (\mathbf{C}_1^{-1},\ldots,\mathbf{C}_n^{-1})$. The MBS velocities are represented by $\mathbf{V} = (\mathbf{V}_1,\ldots,\mathbf{V}_n) \in \left(\mathbb{R}^6\right)^n$. The body-fixed velocities are determined by $\widehat{\mathbf{V}} = q^{-1}\dot{q}$ denoting $\widehat{\mathbf{V}} = (\widehat{\mathbf{V}}_1,\ldots,\widehat{\mathbf{V}}_n)$. The MBS state space is thus the $12\cdot n$-dimensional Lie group

$$S^{\ltimes} := SE(3)^n \times \left(\mathbb{R}^6\right)^n \tag{25}$$

and the MBS state is $X = (q,\mathbf{V}) = (\mathbf{C}_1,\ldots,\mathbf{C}_n,\mathbf{V}_1,\ldots,\mathbf{V}_n) \in S^{\ltimes}$. The multiplication is $X'\cdot X'' = (\mathbf{C}_1'\mathbf{C}_1'',\ldots,\mathbf{C}_n'\mathbf{C}_n'',\mathbf{V}_1'+\mathbf{V}_1'',\ldots,\mathbf{V}_n'+\mathbf{V}_n'')$.
The corresponding Lie algebra is

$$\mathfrak{s}^{\ltimes} := se(3)^n \times \left(\mathbb{R}^6\right)^n, \tag{26}$$

with $x = (\mathbf{V}_1,\ldots,\mathbf{V}_n,\mathbf{A}_1,\ldots,\mathbf{A}_n) \in \mathfrak{s}^{\ltimes}$. The exponential mapping on the state space is

$$\exp x = (\exp\mathbf{V}_1,\ldots,\exp\mathbf{V}_n,\mathbf{A}_1,\ldots,\mathbf{A}_n) \in S^{\ltimes} \tag{27}$$

with (12) with differential $\mathrm{dexp}: \mathfrak{s}^{\ltimes}\times\mathfrak{s}^{\ltimes}\to\mathfrak{s}^{\ltimes}$

$$\mathrm{dexp}_{x'}x'' = (\mathrm{dexp}_{\mathbf{V}_1'}\mathbf{V}_1'',\ldots,\mathrm{dexp}_{\mathbf{V}_n'}\mathbf{V}_n'',\mathbf{A}_1'',\ldots,\mathbf{A}_n''). \tag{28}$$

3.2 Direct Product Group $SO(3)\times\mathbb{R}^3$

When the direct product group is used the MBS configuration $q = (C_1,\ldots,C_n) \in G^{\times}$ belongs to the $6n$-dimensional Lie group

$$G^{\times} := \left(SO(3)\times\mathbb{R}^3\right)^n \tag{29}$$

and possess the inverse $q^{-1} = (C_1^{-1},\ldots,C_n^{-1})$. The hybrid velocity of the MBS is $q^{-1}\dot{q} = ((\widehat{\omega}_1,\mathbf{v}_1^s),\ldots,(\widehat{\omega}_n,\mathbf{v}_n^s))$, and written as vector $V = (\mathbf{V}_1,\ldots,\mathbf{V}_n) \in \left(\mathbb{R}^6\right)^n$ with $\mathbf{V}_i = (\omega_i,\mathbf{v}_i^s)$. Therewith the MBS state space is

$$S^{\times} := \left(SO(3)\times\mathbb{R}^3\right)^n \times \left(\mathbb{R}^6\right)^n \tag{30}$$

with state vector $X = (q,\mathbf{V}) = (C_1,\ldots,C_n,\mathbf{V}_1,\ldots,\mathbf{V}_n) \in S^{\times}$. This is a $12\cdot n$-dimensional Lie group with multiplication $X'\cdot X'' = (C_1'\cdot C_1'',\ldots,C_n'\cdot C_n'',\mathbf{V}_1'+\mathbf{V}_1'',\ldots,\mathbf{V}_n'+\mathbf{V}_n'')$. The Lie algebra of $S^{\times}$ is

$$\mathfrak{s}^{\times} := \left(so(3)\times\mathbb{R}^3\right)^n \times \left(\mathbb{R}^6\right)^n, \tag{31}$$

with elements $x = (\mathbf{V}_1,\ldots,\mathbf{V}_n,\mathbf{A}_1,\ldots,\mathbf{A}_n) \in \mathfrak{s}^{\times}$ where $\mathbf{A}_i = (\alpha_i,\mathbf{a}_i^s)$ represents the body-fixed angular and spatial linear acceleration. The exponential mapping on the ambient state space is

$$\exp x = (\exp\mathbf{V}_1,\ldots,\exp\mathbf{V}_n,\mathbf{A}_1,\ldots,\mathbf{A}_n) \in S^{\times} \tag{32}$$

with (17). The differential $\mathrm{dexp}: \mathfrak{s}^{\times}\times\mathfrak{s}^{\times}\to\mathfrak{s}^{\times}$ is, with (18),

$$\mathrm{dexp}_{x'}x'' = (\mathrm{dexp}_{\mathbf{V}_1'}\mathbf{V}_1'',\ldots,\mathrm{dexp}_{\mathbf{V}_n'}\mathbf{V}_n'',\mathbf{A}_1,\ldots,\mathbf{A}_n). \tag{33}$$

4 Munthe-Kaas Method for Constrained MBS

The Munthe-Kaas (MK) method [8, 10, 11] is a widely used integration scheme for ODE on Lie group that was applied to rigid body dynamics such as [7]. Its appeal stems from its construction since it is a direct extension of the Runge-Kutta method. In order to apply MK a scheme the system equations must be expressed in the form of a first-order ODE on the state space

$$\dot{X} = XF(t,X) \tag{34}$$

with a mapping $F: \mathbb{R}\times S\to\mathfrak{s}$. This is achieved with help of the index 1 system (2). In order to solve for $\dot{X}$, at a given state $X = (q,\mathbf{V}) \in S$, the system (2) must be solved for $\dot{\mathbf{V}}$. It remains to evaluate (2b) for $\dot{q}$. By introducing the mapping

$F(t,X) = (\mathbf{V}, \dot{\mathbf{V}})$, which includes solving for $\dot{\mathbf{V}}$, the system (2) is equivalent to (34) since $XF(t,X) = (q\mathbf{V}, \dot{\mathbf{V}})$. The equations (34) can be regarded as the Boltzmann-Hamel equations on the state space Lie group when its algebra is defined by left trivialization. Evaluation of $XF(t,X)$ thus amounts to solving (2) for $\dot{\mathbf{V}}$ and evaluating (2b). Since both, the rigid body twists (5) and the hybrid velocities (19) are defined by left translation this applies to the $SE(3)$ and the $SO(3) \times \mathbb{R}^3$ formulation as e.g. in [3, 4, 14].
In the MK method solutions are sought of the form $X(t) = X_0 \exp \Phi(t)$. This allows replacing the original system (34) at the integration step i by the system

$$\dot{\Phi}^{(i)} = \operatorname{dexp}^{-1}_{-\Phi^{(i)}} F(t, X_{i-1} \exp \Phi^{(i)}),\ t \in [t_{i-1}, t_i],\ \text{with } \Phi^{(i)}(t_{i-1}) = 0 \tag{35}$$

with initial condition X_{i-1}. Notice the negative sign of $\Phi^{(i)}$ in dexp, which is different from the original MK version. Originally the MK method is derived for right invariant systems, i.e. ODE systems of the form $\dot{X} = F(t,X)X$. Numerically solving (35) yields a solution $\Phi^{(i)}(t_i)$, and thus a solution $X_i := X_{i-1} \exp \Phi^{(i)}(t_i)$ of (34). The $\Phi^{(i)}$ represent local coordinates on the state space defined in a neighborhood of X_{i-1}. The system (35) is solved by an s-stage RK method. This gives rise the corresponding s-stage MK scheme at time step i

$$\begin{aligned} X_i &:= X_{i-1} \exp \Phi^{(i)},\ \Phi^{(i)} := h \sum_{j=1}^{s} b_j k_j \\ k_j &:= \operatorname{dexp}^{-1}_{-\Psi_j} F(t_{i-1} + c_j h, X_{i-1} \exp \Psi_j) \\ \Psi_j &:= h \sum_{l=1}^{j-1} a_{jl} k_l,\ \Psi_1 = 0, \end{aligned} \tag{36}$$

where a_{jl}, b_j, and c_j are the Butcher coefficients of the s-stage RK method, and $k_j, \Psi_j \in \mathfrak{s}$.
It is well-known that the index 1 formulation suffers from constraint violations due to numerical drifts introduced by the numerical update scheme. This is indeed carries over to the introduced Lie group formulation, and the established constraint stabilization methods can be applied. The paper [1] provides a good overview of constraint stabilization methods.

5 Examples

5.1 Heavy Top in Gravity Field

As first example a heavy top is considered, i.e. a single rigid body constrained to rotate about a space-fixed pivot point.
The model concists of a rectangular solid box with side lengths $0.1 \times 0.2 \times 0.4$ m connected to the ground by a speherical joint as shown in figure 1a). A body-fixed reference frame (RFR) is attached at the COM. In the shown reference configuration the RFR is aligned to the space-fixed inertia frame (IFR). Assuming aluminium material the body mass is $m = 21.6$ kg, and its inertia tensor w.r.t. the RFR is $\Theta_0 = \operatorname{diag}(0.36, 0.306, 0.09)$ kg m^2. The position vector of the COM measured from the pivot point expressed in the body-fixed reference frame is denoted with $\mathbf{r}_0 = (0.5, 0, 0)$ m. The configuration of the reference frame is represented by $C = (\mathbf{R}, \mathbf{r}^s)$.

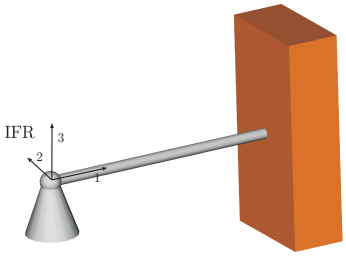

FIGURE 1. Model of a heavy top.

Motion Equations in Body-Fixed Representation The pivot imposes the geometric constraints

$$\mathbf{g}(C) = \mathbf{r}_0 - \mathbf{R}^T \mathbf{r}^s = \mathbf{0}. \tag{37}$$

Time differentiation yields the velocity and acceleration constraints

$$\left(\widehat{\mathbf{R}^T \mathbf{r}^s}\ \mathbf{I}\right) \begin{pmatrix} \omega \\ \mathbf{v} \end{pmatrix} = \mathbf{J}\mathbf{V} = \mathbf{0}, \quad \left(\widehat{\mathbf{R}^T \mathbf{r}^s}\ \mathbf{I}\right) \begin{pmatrix} \dot{\omega} \\ \dot{\mathbf{v}} \end{pmatrix} = -\widehat{\omega}\widehat{\omega}\mathbf{r}_0 + \widehat{\omega}\mathbf{v} \tag{38}$$

where the body-fixed twist is denoted $\mathbf{V} = (\omega, \mathbf{v})$. These together with the body-fixed Newton-Euler equations w.r.t. to the COM give rise to the system (2)

$$\begin{pmatrix} \Theta_0 & \mathbf{0} & -\widehat{\mathbf{r}}_0 \\ \mathbf{0} & m\mathbf{I} & \mathbf{I} \\ \widehat{\mathbf{r}}_0 & \mathbf{I} & \mathbf{0} \end{pmatrix} \begin{pmatrix} \dot{\omega} \\ \dot{\mathbf{v}} \\ \lambda \end{pmatrix} = \begin{pmatrix} \mathbf{M} - \widehat{\omega}\Theta_0\omega \\ \mathbf{F} - m\widehat{\omega}\mathbf{v} \\ -\widehat{\omega}\widehat{\omega}\mathbf{r}_0 + \widehat{\omega}\mathbf{v} \end{pmatrix} \tag{39}$$

where (37) is assumed satisfied. $\mathbf{F}$ and $\mathbf{M}$ is the external force and torque, respectively, acting on the COM represented in the body-fixed frame.

Motion Equations in Hybrid Velocity Representation In hybrid velocity representation $(\omega, \mathbf{v}^s)$ the geometric constraints (37) gives rise to the following velocity and acceleration constraints, respectively,

$$\left(\mathbf{R}\widehat{\mathbf{r}}_0\ \mathbf{I}\right) \begin{pmatrix} \omega \\ \mathbf{v}^s \end{pmatrix} = \mathbf{0}, \quad \left(\mathbf{R}\widehat{\mathbf{r}}_0\ \mathbf{I}\right) \begin{pmatrix} \dot{\omega} \\ \dot{\mathbf{v}}^s \end{pmatrix} = \mathbf{R}\widehat{\omega}\widehat{\omega}\mathbf{r}_0. \tag{40}$$

The Newton-Euler equations w.r.t. to COM in hybrid representation yields

$$\begin{pmatrix} \Theta_0 & \mathbf{0} & (\mathbf{R}\widehat{r}_0)^T \\ \mathbf{0} & m\mathbf{I} & \mathbf{I} \\ \mathbf{R}\widehat{\mathbf{r}}_0 & \mathbf{I} & \mathbf{0} \end{pmatrix} \begin{pmatrix} \dot{\omega} \\ \dot{\mathbf{v}}^s \\ \lambda \end{pmatrix} = \begin{pmatrix} \mathbf{M} - \widehat{\omega}\Theta_0\omega \\ \mathbf{F}^s \\ \mathbf{R}\widehat{\omega}\widehat{\omega}\mathbf{r}_0 \end{pmatrix}. \qquad (41)$$

$\mathbf{F}^s$ is the external force acting on the COM represented in the spatial frame.

Numerical Results No gravity or external forces and torques are present, i.e. $\mathbf{M} = \mathbf{F} = \mathbf{0}$. The integration step size is $\Delta t = 10^{-3}$ s. In the reference configuration the top has the same orientation as the inertial frame shown in figure 1a). The initial angular velocity was set to $\omega_0 = (0, 20\pi, 10\pi)$ rad/s so that the top will perform a spatial rotation.
Figure 2 shows the deviation of the location of the COM reference frame for numerical solutions obtained with the $SE(3)$ and $SO(3) \times \mathbb{R}^3$ formulation, respectively. The $SE(3)$ integration yields the correct result within the computation accuracy while the $SO(3) \times \mathbb{R}^3$ formulation shows significant drifts.

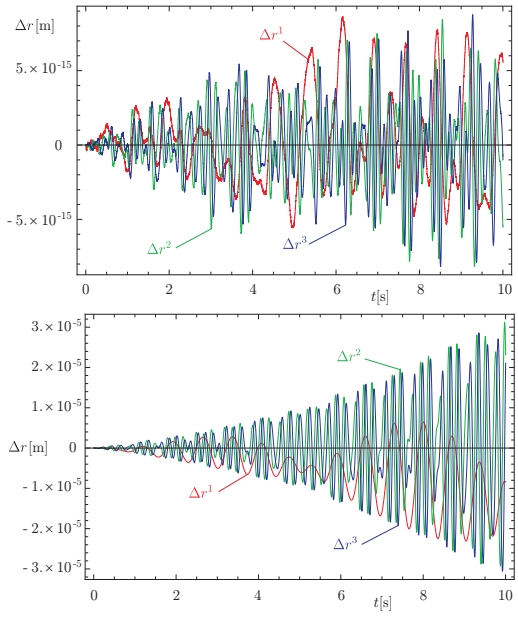

FIGURE 2. Drift of rotation center for integration on a) $SE(3)$, and b)$SO(3) \times \mathbb{R}^3$.

A reference trajectory was numerically determined by integrating the dynamic Euler-equations in quaternion parameterization using a RK4 integration scheme with variable step size and relative and absolute accuracy goal of 10^{-6} and 10^{-9}, respectively. Figure 3 shows the kinetic energy drift for integration on $SE(3)$ relative to the initial value $T_0 = 13.97$ kJ. This is two orders of magnitude smaller than the drift of the $SO(3) \times \mathbb{R}^3$ formulation (fig. 3b)).

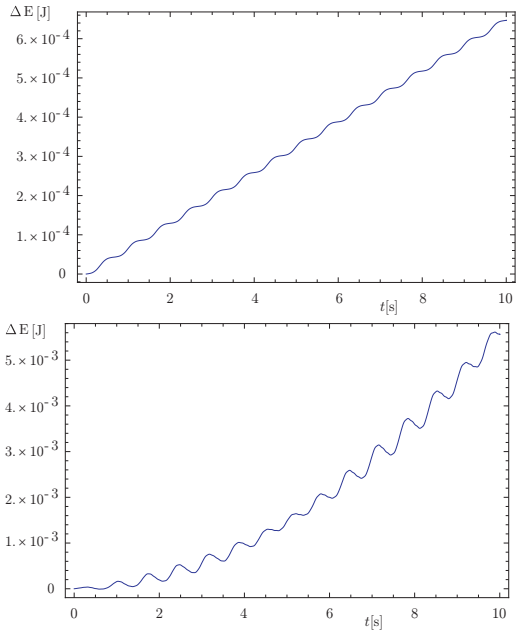

FIGURE 3. Drift of kinetic energy for a) $SE(3)$ and b) $SO(3) \times \mathbb{R}^3$ formulation.

5.2 Spherical Double Pendulum in Gravity Field

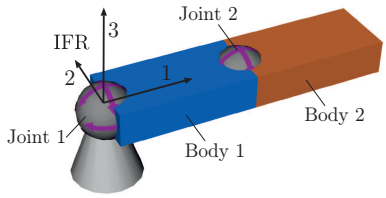

FIGURE 4. Spherical double pendulum.

The double pendulum is considered consisting of two slender rigid bodies as shown in figure 1b). The two bodies are interconnected and the pendulum as a whole is connected to the ground by spherical joints. The two links are flat boxes with side length a, b, c along the axes of the COM reference frame. Both have the same dimension with lengths $a = 0.2\,\text{m}, b = 0.1\,\text{m}, c = 0.05\,\text{m}$. The configuration of the system is represented by $C_1 = (\mathbf{R}_1, \mathbf{r}_1^s)$ and $C_2 = (\mathbf{R}_2, \mathbf{r}_2^s)$. The two links are subject to the geometric constraints

$$\begin{aligned} \mathbf{g}_1(C_1) &= \mathbf{R}_1\mathbf{r}_0 + \mathbf{r}_1^s = \mathbf{0} \\ \mathbf{g}_2(C_1, C_2) &= \mathbf{R}_1\mathbf{r}_{10} + \mathbf{r}_1^s - \mathbf{R}_2\mathbf{r}_{20} - \mathbf{r}_2^s = \mathbf{0} \end{aligned} \qquad (42)$$

where $\mathbf{r}_{i0}, i = 1, 2$ is the position vector from the COM frame on body i to the spherical joint connecting the two links, expressed in the COM frame. $\mathbf{r}_0$ is the position vector from the COM frame on body 1 to the spherical joint connecting it to the ground expressed in this COM frame. Denote with Θ_{i0} the inertia tensor of body i w.r.t. the COM frame, and with m_i its mass.

Motion Equations in Body-Fixed Representation The velocity and acceleration constraints corresponding to (42), in terms of body-fixed twists $\mathbf{V}_1, \mathbf{V}_2 \in se(3)$, are

$$\mathbf{0} = \begin{pmatrix} \widehat{\mathbf{r}}_0 & -\mathbf{I} & \mathbf{0} & \mathbf{0} \\ \mathbf{R}_1\widehat{\mathbf{r}}_{10} & -\mathbf{R}_1 & -\mathbf{R}_2\widehat{\mathbf{r}}_{20} & \mathbf{R}_2 \end{pmatrix} \begin{pmatrix} \omega_1 \\ \mathbf{v}_1 \\ \omega_2 \\ \mathbf{v}_2 \end{pmatrix} = \mathbf{J}\mathbf{V} \tag{43}$$

$$\mathbf{J}\dot{\mathbf{V}} = \begin{pmatrix} \widehat{\omega}_1\mathbf{v}_1 + \widehat{\omega}_1\widehat{\omega}_1\mathbf{r}_0 \\ \mathbf{R}_1\widehat{\omega}_1\widehat{\omega}_1\mathbf{r}_{10} - \mathbf{R}_2\widehat{\omega}_2\widehat{\omega}_2\mathbf{r}_{20} + \mathbf{R}_1\widehat{\omega}_1\mathbf{v}_1 - \mathbf{R}_2\widehat{\omega}_2\mathbf{v}_2 \end{pmatrix} \tag{44}$$

Using a reference frame at the COM yields

$$\begin{pmatrix} \Theta_{10} & \mathbf{0} & \mathbf{0} & \mathbf{0} & -\widehat{\mathbf{r}}_0 & -\widehat{\mathbf{r}}_{10}\mathbf{R}_1^T \\ \mathbf{0} & m_1\mathbf{I} & \mathbf{0} & \mathbf{0} & -\mathbf{I} & -\mathbf{R}_1^T \\ \mathbf{0} & \mathbf{0} & \Theta_{20} & \mathbf{0} & \mathbf{0} & \widehat{\mathbf{r}}_{20}\mathbf{R}_2^T \\ \mathbf{0} & \mathbf{0} & \mathbf{0} & m_2\mathbf{I} & \mathbf{0} & \mathbf{R}_2^T \\ \widehat{\mathbf{r}}_0 & -\mathbf{I} & \mathbf{0} & \mathbf{0} & \mathbf{0} & \mathbf{0} \\ \mathbf{R}_1\widehat{\mathbf{r}}_{10} & -\mathbf{R}_1 & -\mathbf{R}_2\widehat{\mathbf{r}}_{20} & \mathbf{R}_2 & \mathbf{0} & \mathbf{0} \end{pmatrix} \begin{pmatrix} \dot{\omega}_1 \\ \dot{\mathbf{v}}_1 \\ \dot{\omega}_2 \\ \dot{\mathbf{v}}_2 \\ \lambda_1 \\ \lambda_2 \end{pmatrix} = \begin{pmatrix} -\widehat{\omega}_1\Theta_{10}\omega_1 \\ \mathbf{F}_1 - m_1\widehat{\omega}_1\mathbf{v}_1 \\ -\widehat{\omega}_2\Theta_{20}\omega_2 \\ \mathbf{F}_2 - m_2\widehat{\omega}_2\mathbf{v}_2 \\ * \\ ** \end{pmatrix} \tag{45}$$

where $*$ and $**$ are the terms in the two rows of the right hand side of (44). Since only gravity forces act on the systems the body-fixed forces are $\mathbf{F}_i = \mathbf{R}_i^T\mathbf{g}^s$, where $\mathbf{g}^s = (0,0,-g)$ is the gravity vector w.r.t. space-fixed frame. The Lagrange multiplier $\lambda_i \in \mathbb{R}^3$ is the reaction force in joint i.

Motion Equations in Hybrid Velocity Representation With hybrid velocities $\mathbf{V}_i = (\omega_i, \mathbf{v}_i^s)$ the velocity and acceleration constraints are

$$\mathbf{0} = \begin{pmatrix} \mathbf{R}_1\widehat{\mathbf{r}}_0 & -\mathbf{I} & \mathbf{0} & \mathbf{0} \\ \mathbf{R}_1\widehat{\mathbf{r}}_{10} & -\mathbf{I} & -\mathbf{R}_2\widehat{\mathbf{r}}_{20} & \mathbf{I} \end{pmatrix} \begin{pmatrix} \omega_1 \\ \mathbf{v}_1 \\ \omega_2 \\ \mathbf{v}_2 \end{pmatrix} = \mathbf{J}\mathbf{V} \tag{46}$$

$$\mathbf{J}\dot{\mathbf{V}} = \begin{pmatrix} \mathbf{R}_1\widehat{\omega}_1\widehat{\omega}_1\mathbf{r}_0 \\ \mathbf{R}_1\widehat{\omega}_1\widehat{\omega}_1\mathbf{r}_{10} - \mathbf{R}_2\widehat{\omega}_2\widehat{\omega}_2\mathbf{r}_{20} \end{pmatrix}. \tag{47}$$

The index 1 motion equations are, with force vectors $\mathbf{F}_i^s = \mathbf{g}^s$,

$$\begin{pmatrix} \Theta_{10} & \mathbf{0} & \mathbf{0} & \mathbf{0} & -\widehat{\mathbf{r}}_0\mathbf{R}_1^T & -\widehat{\mathbf{r}}_{10}\mathbf{R}_1^T \\ \mathbf{0} & m_1\mathbf{I} & \mathbf{0} & \mathbf{0} & -\mathbf{I} & -\mathbf{I} \\ \mathbf{0} & \mathbf{0} & \Theta_{20} & \mathbf{0} & \mathbf{0} & \widehat{\mathbf{r}}_{20}\mathbf{R}_2^T \\ \mathbf{0} & \mathbf{0} & \mathbf{0} & m_2\mathbf{I} & \mathbf{0} & \mathbf{I} \\ \mathbf{R}_1\widehat{\mathbf{r}}_0 & -\mathbf{I} & \mathbf{0} & \mathbf{0} & \mathbf{0} & \mathbf{0} \\ \mathbf{R}_1\widehat{\mathbf{r}}_{10} & -\mathbf{I} & -\mathbf{R}_2\widehat{\mathbf{r}}_{20} & \mathbf{I} & \mathbf{0} & \mathbf{0} \end{pmatrix} \begin{pmatrix} \dot{\omega}_1 \\ \dot{\mathbf{v}}_1^s \\ \dot{\omega}_2 \\ \dot{\mathbf{v}}_2^s \\ \lambda_1 \\ \lambda_2 \end{pmatrix} = \begin{pmatrix} -\widehat{\omega}_1\Theta_{10}\omega_1 \\ \mathbf{F}_1^s \\ -\widehat{\omega}_2\Theta_{20}\omega_2 \\ \mathbf{F}_2^s \\ * \\ ** \end{pmatrix}$$

The terms $*$ and $**$ in the two rows of the right hand side of (47).

Numerical Results In the initial configuration $C_1(0) = (\mathbf{I}, (a_1/2, 0, 0))$, $C_2(0) = (\mathbf{I}, (a_1 + a_2/2, 0, 0))$ the pendulum is aligned along the space-fixed x-axis as shown in figure 1b). The initial velocities are set to $\omega_{10} = (10, 0, 0)$ rad/s and $\omega_{20} = (10\pi, 10\pi, 20\pi)$ rad/s. The pendulum is moving in the gravity field. A time step size of $\Delta t = 10^{-3}$s is used in the MK method (36). Figure 5 and 6 reveal a generally better performance of the $SE(3)$ formulation. It also reveals that the constraint violation is more pronounced when it is due to the relative motion of two screw motions, which explains that the violation in joint 2 is higher than that in joint 1. The total energy drift is comparable for both formulations (figure 7).

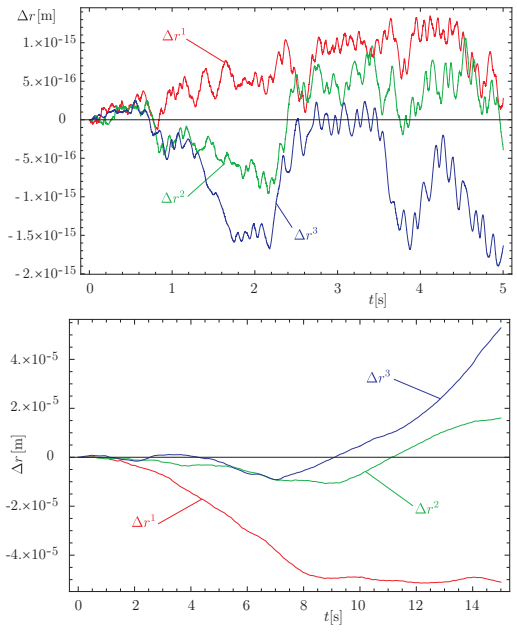

FIGURE 5. Violation of geometric constraints of joint 1 when integrating the $SE(3)$ (a), and $SO(3) \times \mathbb{R}^3$ (b) formulation.

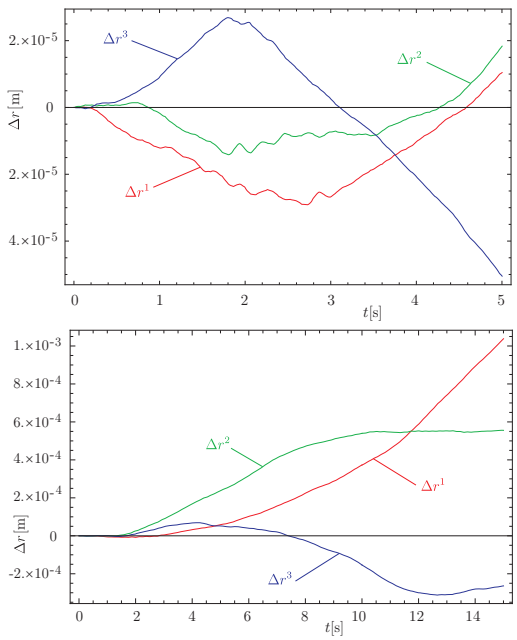

FIGURE 6. Violation of geometric constraints of joint 2 when integrating a) the $SE(3)$, and b) $SO(3) \times \mathbb{R}^3$ formulation.

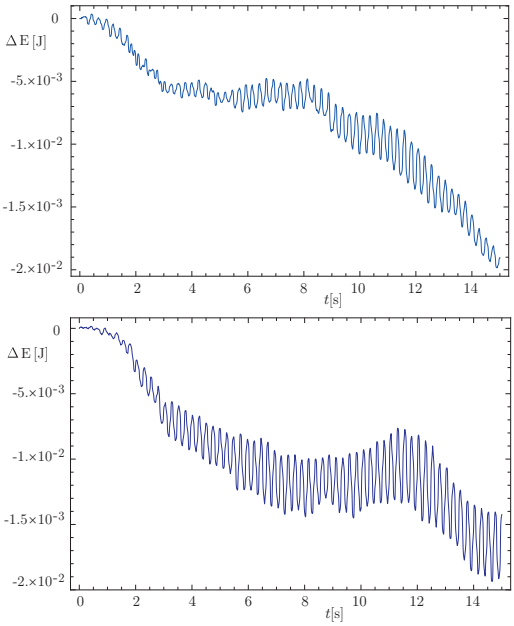

FIGURE 7. Drift of total energy for a) the $SE(3)$, and b) $SO(3)\times\mathbb{R}^3$.

5.3 Interconnected Floating Bodies

Consider the situation in figure 8 where the two bodies in the above spherical double pendulum mutually connected but are not connected to the ground. That is, the two bodies, connected by one spherical joint, are free floating, and no gravity is assumed. The motion equations are the same as those of the spherical double pendulum above except that the first constraint in (43),(44), and (46),(47), respectively, are removed.

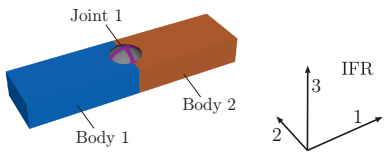

FIGURE 8. Two floating bodies connected by spherical joint.

Again the initial configuration is such that the bodies are horizontally alligned. The initial angular velocities are $\omega_{10} = (0,0,-10)$ rad/s and $\omega_{20} = (1,-1,2\pi)$ rad/s.

The numerical results obtained by the Lie group integration schemes are shown in figure 9. Apparently for this example both formulations perform similarly regarding constraint satisfaction. Also the kinetic energy drifts are similar as shown in 10.

This example differs from the previous ones in that the constraint violation is caused by the spatial motion of two interconnected bodies rather then by the motion of one body that is connected to the ground.

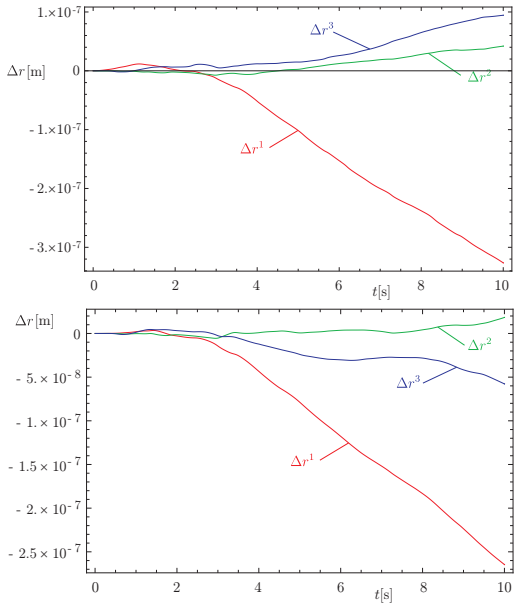

FIGURE 9. Drift of rotation center for integration on a) $SE(3)$, and b) $SO(3)\times\mathbb{R}^3$.

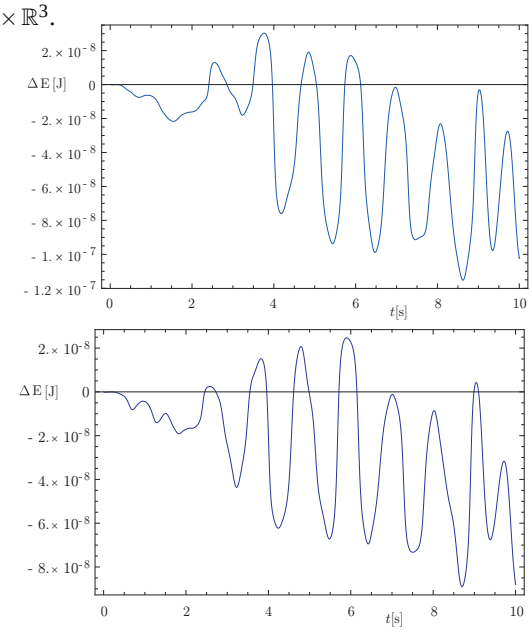

FIGURE 10. Drift of kinetic energy for a) $SE(3)$ and b) $SO(3)\times\mathbb{R}^3$ formulation.

5.4 Closed Loop Spherical 3-Bar Linkage

As final example the closed-loop three-bar mechanism in figure 11 is considered. Due to space limitations the motion equation are not given here. The results in figure 12-14 confirm that again that the constraints are perfectly satisfied if only the motion of one body is to be estimated, i.e. the base joints. The constraint violation of joint 2 connecting the two bodies is similar for both formulations. Also the energy drift of both formulations is simi-

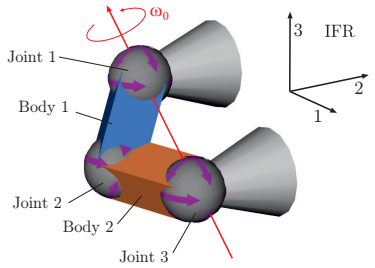

FIGURE 11. Closed loop 3-bar linkage.

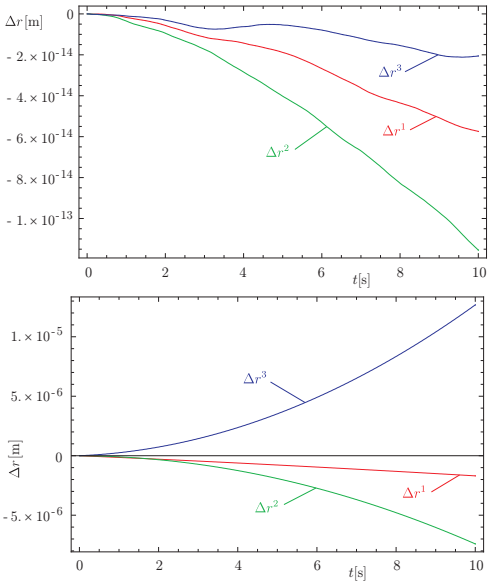

a)

b)

FIGURE 12. Violation of geometric constraints of joint 1 when integrating the $SE(3)$ (a), and $SO(3) \times \mathbb{R}^3$ (b) formulation.

lar (fig. 15).

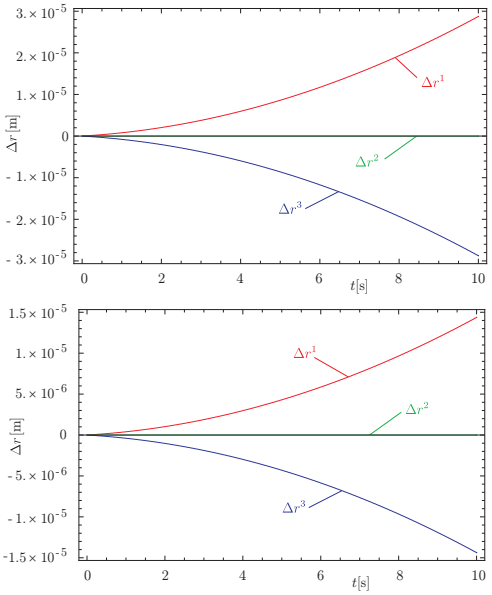

a)

b)

FIGURE 13. Violation of geometric constraints of joint 2 when integrating the $SE(3)$ (a), and $SO(3) \times \mathbb{R}^3$ (b) formulation.

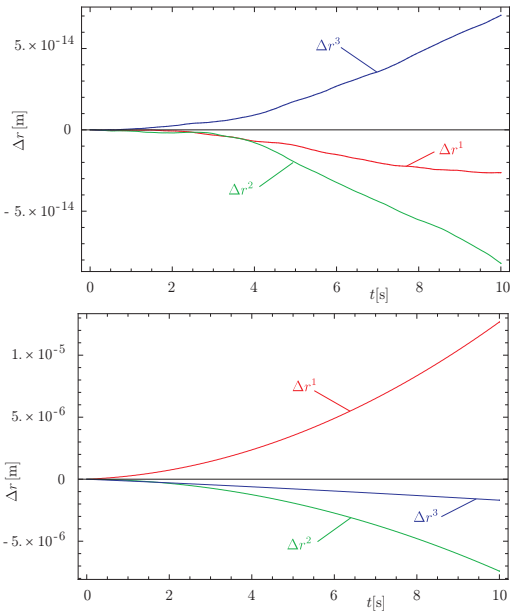

a)

b)

FIGURE 14. Violation of geometric constraints of joint 3 when integrating the $SE(3)$ (a), and $SO(3) \times \mathbb{R}^3$ (b) formulation.

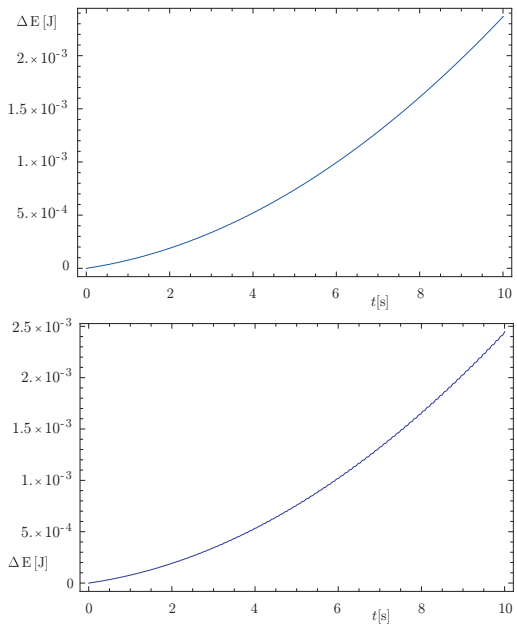

a)

b)

FIGURE 15. Drift of total energy for a) the $SE(3)$, and b) $SO(3) \times \mathbb{R}^3$.

6 Discussion and Conclusion

A generic rigid body motion is a screw motion, and the corresponding velocity is a proper twist. Consequently the finite motion of a body is best approximated from its instantaneous twist as finite screw motion. As the actual cause of the body twist is irrelevant this applies equally to a free floating body as well as to a holonomically and scleronomically constrained body, in particular when jointly connected to the ground. From a computational point of view the numerical representation of screw motions is crucial. Generally, the Lie group $SE(3)$ represents rigid body motions and is the proper rigid body configuration space allowing for the reconstruction of finite motions from velocities. Nevertheless, frequently the direct product group $SO(3) \times \mathbb{R}^3$ is employed as configuration space. The latter does allow for representing rigid body configurations but not motions, however. The question arises whether this is significant for the numerical simulation. Lie group integration schemes take explicitly into account the configuration space manifold, so that the numerical update within the integration scheme is different for the two configuration spaces. With the above said it is clear that the actual performance of the integration scheme depends on the underlying configuration space Lie group, and it may be conjectured that the $SE(3)$ formulation outperforms the $SO(3) \times \mathbb{R}^3$ formulation.

In this paper the accuracy of numerical Munthe-Kaas integration schemes applied to the two formulations is investigated. The results confirm that the $SE(3)$ formulation yields the best overall performance. In particular, since rigid body motions are described relative to an inertial reference frame, the $SE(3)$ formulation allows for perfect reconstruction of the motion of a constrained rigid body if its motion is constrained to a proper motion subgroup. This is the case when a rigid body is connected to the ground (or to another slowly moving body) by a lower pair. In the general case of rigid bodies connected by lower pairs their relative motion belongs to a motion subgroup but their absolute motion does not. In these cases also the reconstruction as screw motion of the individual bodies from first-order motions cannot capture the interdependence of their finite motions, and both formulations perform equally.

In summary the $SE(3)$ update scheme performs generally as good as the $SO(3) \times \mathbb{R}^3$ formulation while it outperforms the latter when bodies are constrained to a stationary body, in particular the ground.

This advantage is owed to an increase in cmplexitiy since the $SE(3)$ update scheme is computationally more complex than the standard direct product $SO(3) \times \mathbb{R}^3$ update. In order to minimize the complexity of the integration scheme, for a given problem, the configuration space can be introduced so that the $SE(3)$ is used as configuration space where appropriate and $SO(3) \times \mathbb{R}^3$ otherwise. Such tailored designation of configuration spaces will be part of furure work aiming on integration schemes that minimize constraint violation in numerical MBS models. This paper addressed the performance of MK integration methods. To complete this study the effect of different configuration space for other Lie group integration schemes will be investigated in future.

REFERENCES

[1] W. Blajer: Methods for constraint violation suppression in the numerical simulation of constrained multibody systems – A comparative study, Comput. Methods Appl. Mech. Engrg. Vol. 200, 2011, pp. 1568–1576

[2] A. Bottema, B. Roth: Theoretical Kinematics, North-Holland, 1979

[3] O. Brüls, A. Cardona: On the Use of Lie Group Time Integrators in Multibody Dynamics, J. Comput. Nonlinear Dynam. 5(3) 2010

[4] O. Brüls, A. Cardona, M. Arnold: Lie group generalized-alpha time integration of constrained flexible multibody systems, Mech. Mach. Theory 48, 2012, 121-137

[5] H. Bruyninckx, J. De Schutter: Symbolic differentiation of the velocity mapping for a serial kinematic chain, Mech. Mach. Theory 31(2) 1996, 135-148

[6] F. Bullo, R.M. Murray: *Proportional Derivative (PD) Control on the Euclidean group*, CDS technical report 95-010, 1995

[7] E. Celledoni, B. Owren: *Lie Group Methods for Rigid Body Dynamics and Time Integration on Manifolds*, Computer Methods in Applied Mechanics and Engineering 19, 1999, 421-438

[8] E. Hairer, C. Lubich and G. Wanner: Geometric Numerical Integration, Springer, 2006

[9] P. Krysl, L. Endres: Explicit Newmark/Verlet algorithm for time integration of the rotational dynamics of rigid bodies, Int. J. Numer. Meth. Engng. 62, 2005, 2154-2177

[10] H. Munthe-Kaas, *Runge Kutta methods on Lie groups*, BIT, 38(1) 1998, 92-111

[11] H. Munthe-Kaas, *High order Runge-Kutta methods on manifolds*, Appl. Numer. Math. 29, 1999, 115-127

[12] R.M Murray, Z. Li, S. S. Sastry: *A mathematical Introduction to robotic Manipulation*, CRC Press, 1993

[13] J.M. Selig, *Geometrical Methods in Robotics*, Springer, New York, 1996.

[14] Z. Terze, A. Müller, D. Zlatar: Lie-Group integration method for constrained multibody systems in stabilized index 1 form, Multibody System Dynamics, submitted, 2011